18.4

AIRCRAFT MEASUREMENTS AND SIMULATIONS OF MOUNTAIN WAVES OVER MONT BLANC

Samantha Smith *, A. S. Broad
Met Office, Bracknell, Berkshire U.K.

1. INTRODUCTION

On the morning of 2 November 1999 (during MAP) the Met Office C130, the NCAR Electra and the DLR Falcon flew a joint aircraft mission over Mont Blanc to observe lee-waves trapped in the troposphere by the jet stream, which produced strong uni-directional south-westerly flow and positive wind-shear. Each aircraft flew repeat legs along a specified flight track oriented to within 10° of the mean wind direction, enabling the temporal variation in the wave-field to be captured. This paper examines the effect such temporal variations had on the momentum fluxes through analysis of the aircraft and sonde data. Also, a high horizontal resolution (1km), 3-D, non-hydrostatic simulation has been carried out using smoothed orography from a 2km dataset. This simulation is being used to aid understanding of the observations, and in particular to investigate the horizontal variability in the waves and their momentum fluxes.

2. RESULTS

Figure 1 shows the vertical displacements calculated from the vertical velocities observed by each aircraft after detrending and filtering to remove scales smaller than 2km and scales larger than 30km. The highest flight levels are not shown as the waves were trapped below 11km. A cross-section through the orography along the flight track shows the part of the Mont Blanc massif which penetrates above a stagnant layer, which was present below 2.5km, into the fast moving flow aloft. The stagnant layer, caused by blocking by the surrounding mountains had the effect of: (1) reducing the effective mountain height and therefore the magnitude of the gravity waves and (2) absorbing the downward propagating waves which were reflected from the trapping level (Smith et al, 2002). The waves are therefore of moderate amplitude and extend only two wavelengths downstream. The dominant wavelength increases with height due

*Corresponding author address: Samantha A Smith, Met Office, Bracknell, Berkshire, RG12 2SZ, U.K.; email: samantha.smith@metoffice.com

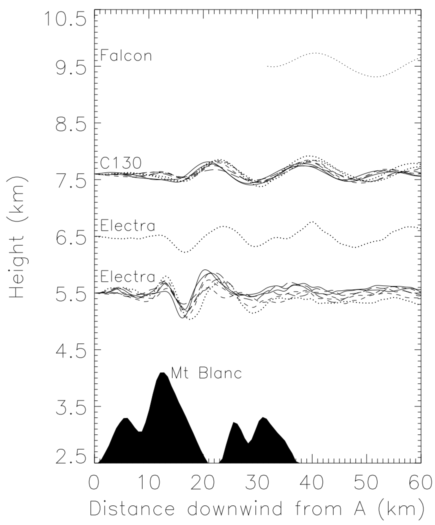

Figure 1: Vertical displacements observed by all three aircraft and a cross-section through the orography along the flight track which penetrates above the stagnant layer

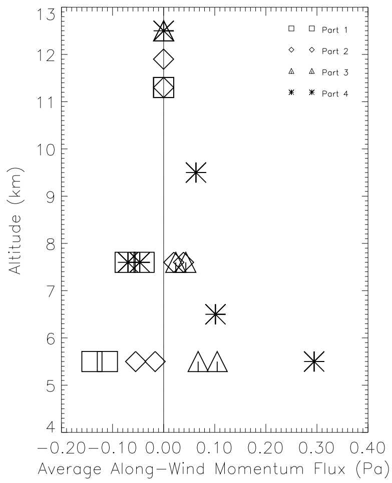

Figure 2: Observed profile of along-wind momentum fluxes averaged over 60km transects

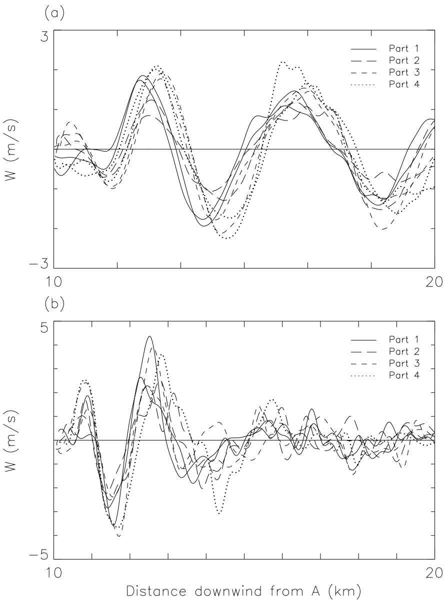

Figure 3: Vertical wind velocity w observed at (a) 7.6km and (b) 5.5km with solid/dotted lines indicating the earliest/latest runs

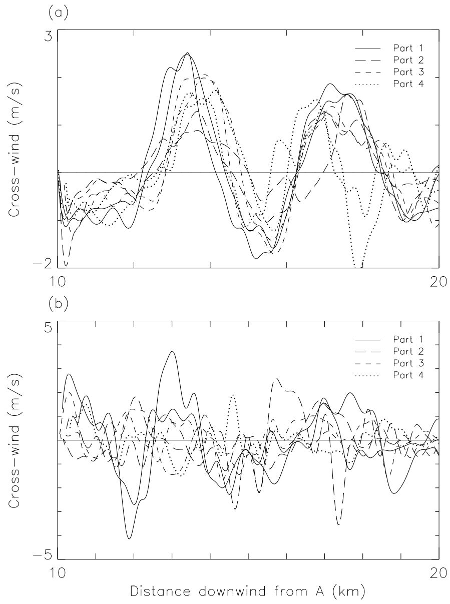

Figure 5: As for Figure 3 but for the cross-wind component v (m s^{-1})

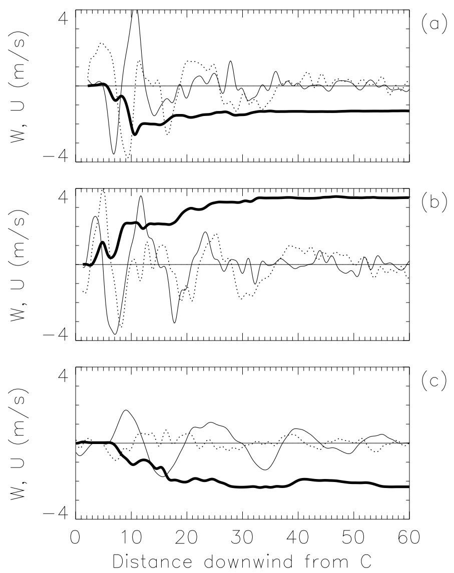

Figure 4: Time-series of w (solid), u (dotted) and F_{tot} (thick) for (a) the first C130 run, (b) the first Electra run at 5.5km and (c) the last Electra run at 5.5km.

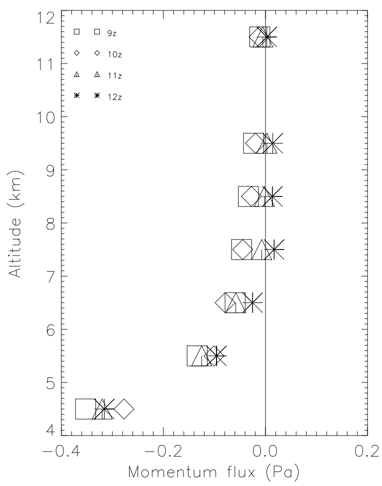

Figure 6: Model predicted along-wind momentum flux profile obtained using data extracted along the aircraft flight track

to the decreasing Scorer parameter. At first sight the wave field appears fairly stationary throughout the 3 hour flight period.

Along the flight track the model agrees fairly well with the observed wave field over Mont Blanc. The lower wavelength is 6-8km as observed, but the magnitudes in w are underestimated due to insufficient horizontal resolution. The upper tropospheric wavelength is slightly underestimated but the magnitudes agree with the observations.

2.1 Momentum Fluxes

A cumulative total momentum flux F_{tot} was calculated along each flight leg starting from a position C (10km downstream from A and just upwind of Mont Blanc) using the filtered and detrended velocities. The average momentum flux over a distance L is given by

$$F_{av} = \frac{F_{tot}}{L} = \frac{\rho \ \Sigma w_i u_i \ \Delta x}{l_i} \qquad (1)$$

where ρ is the mean density, Δx is the horizontal distance between data-points with respect to the ground, w_i is the vertical wind velocity perturbation at position i and u_i is the horizontal wind velocity perturbation in the direction of the mean wind. Data-point i is a distance of l_i from C. A value of 60km was chosen for L to include all of the wave signature along the track without including too much of the time-series downwind. The resulting profile of the vertical flux of along-wind momentum is plotted in figure 2 with different symbols representing different time periods. The scatter in the momentum fluxes is very large, particularly at the lowest flight level, and is much larger than would be expected from observational errors. The scatter results in a flight average momentum flux which is close to zero. However, the variability in the momentum fluxes is real and is well correlated with the variability in the wave magnitude observed in the vertical velocities, as shown in Figure 3. The solid lines show the earliest runs, which correlate with the squares in Figure 2, while the dotted lines show the latest runs, which correlate with the asterisks in Figure 2. At the start of the flight the waves in w and their momentum fluxes were of large magnitude, but they were smaller mid-flight. By the end of the flight the waves and the fluxes had grown to larger magnitudes again.

At the C130 flight level of 7.6km, the momentum fluxes for runs with larger waves have negative momentum fluxes, with the largest contribution coming from the primary wave directly over the mountain as suggested by Bretherton (1969). This can be seen in Figure 4 (c) where a negative perturbation in u (thin dotted line) is correlated with the first peak in w (thin solid line). The value of F_{tot} is shown as the solid black line, which converges to a constant value beyond a distance of 40km downstream from C. The fact that these waves are fairly weakly trapped means that the lee-waves downstream also contribute a negative momentum flux. These downstream lee-waves are not well defined in u, although they show a large signature in the cross-wind component, v, as shown in Figure 5(a). Quite why v should exhibit such large waves is not yet understood. Data was extracted from the simulation along a number of cross-sections parallel to the original flight track, but there is no line where the perturbations in v are greater than in u. The largest perturbations in v are found displaced from the centre of Mont Blanc, where the perturbations in u and v are at best comparable.

At the Electra flight level of 5.5km the scatter in the run average momentum fluxes is very large, varying from large negative values at the start of the flight through to large positive values by the end of the flight. Figures 4(a) and 4(b) are the same as Figure 4(c) but for the first and last Electra runs at 5.5km respectively. The phase relationship between w and u indicates whether the wave is propagating upwards (180°) or downwards (0°). A perfectly trapped wave is the superposition of upward and downward propagating waves which are generally propagating downstream and the phase relationship between w and u is 90°. Figure 4(a) shows large waves in both w and u which have a phase relationship somewhere between 90 and 180° due to the dominance of the upward propagating wave forced by the mountain. The resulting negative wave momentum flux is large and concentrated in the region directly over Mont Blanc. Figure 4(b) also shows large wave magnitudes in both w and u but the phase relationship is between 90 and 0°, indicating that the downward propagating wave dominates over the incident wave forced by the mountain. This results in a large positive momentum flux, the reasons for which are under investigation.

Generally the run averaged momentum fluxes observed in this case are comparable to other values found from aircraft observations in mountain waves. Brown (1983), who analysed aircraft observations in trapped lee-waves over the UK, found that only 2 of the 5 flights analysed yielded momentum fluxes of magnitude larger than 0.1 Pa, and that these were the weakly trapped lee-waves of longer horizontal wavelength. The trapped lee-waves observed by

Brown extended far downstream and averages were calculated over the full 200km length of each run. The limited extent of the lee-waves in the present case makes the choice of averaging length much more difficult. The lee-waves produce large momentum fluxes which are highly localised in space and averaging over a longer transect reduces the run average. If, for example, the averages at the Electra flight level of 5.5km of were taken over the first 12km downstream from C, then the average momentum fluxes would vary in time from -0.7 to +0.9 Pa (increased by a factor of 3).

Data was extracted from the simulated wind field along a cross section oriented along the flight track. Time-series extracted from this cross section along lines of constant height above sea level were used to calculate the average momentum fluxes as for the aircraft data with an averaging length L of 60km. This was done hourly between 9z and 12z and the results are shown in Figure 6. The 9z simulated momentum fluxes close to the aircraft flight levels of 5.5 and 7.6km are comparable to the observations at the start of the flight. However there is less temporal variability during the morning and no positive momentum fluxes in the lower troposphere. Examination of the w, u and F_{tot} time-series show that the negative momentum flux is dominated in the upper troposphere by the primary wave over Mont Blanc and the flux at 5.5km is large and highly localised in space as in the observed time-series.

3. CONCLUSIONS

A small amplitude quasi-stationary lee-wave field was observed over Mont Blanc on the morning of 2 November 1999 during MAP. The scatter in the run-average momentum fluxes was large, with a flight average close to zero. On closer inspection it was found that the wave magnitude in the vertical wind velocities varied by as much as 50% of its original value, resulting in temporal variability in the average momentum fluxes at each height. The primary wave immediately above the mountain dominated the negative momentum fluxes in the upper tropospheric waves, although the lee-waves downstream also contributed to the negative momentum flux due to the leakage of wave energy into the stratosphere. For runs when the wave magnitude was smaller the waves no longer dominated the run averages and small positive values were found due to other variations in the winds. In the lower troposphere the picture was much more complicated and the scatter in the momentum fluxes was much larger, varying from a large negative value through to a large positive value. The positive momentum flux observed at the end of the flight suggests dominance of the reflected wave at that time, and the reasons for this are being investigated. A high horizontal resolution, 3-D, non-hydrostatic simulation over real orography has been produced which agrees fairly well with the observations except for an underestimation of the lower tropospheric wave magnitude and of the upper tropospheric wavelength. The momentum flux profile along the aircraft transect looks similar to the observations at the start of the flight but does not reproduce the large positive momentum fluxes observed by the Electra.

4. REFERENCES

Bretherton, F. P., 1969. Momentum transport by gravity waves. *Quart. J. R. Met. Soc.*, **95**, 213–243.

Brown, P. R. A., 1983. Aircraft measurements of mountain waves and their associated momentum flux over the British Isles. *Quart. J. R. Met. Soc.*, **109**, 849–865.

Smith, R. B., Skubis, S., Doyle, J. D., Broad, A., and H. Volkert, 2002: Gravity waves over Mt. Blanc. Accepted for publication. *J.A.S.*